EFFECT OF TOPOGRAPHY AND SUBSURFACE INHOMOGENEITY ON SEISMIC SV WAVES AND RAYLEIGH WAVES

A. Ohtsuki (I)
H. Yamahara (II)
Presenting Author : A. Ohtsuki

Summary

The effect of topography and subsurface inhomogeneity on surface motion is investigated in cases of incident SV waves and Rayleigh waves. Several types of topography, such as cliffs with and without a soft layer at the foot of the slope are considered. Computations are made using a new hybrid method combining a particle model with a finite element method. It is found that the influences of irregular ground on SV waves and Rayleigh waves differ depending on the relationship between the incident wavelength and the geometrical dimensions of the irregular ground and these influences cannot be ignored.

Introduction

It is often observed that earthquake damages concentrate in certain regions. For instance in 1968 Tokachi-oki Earthquake in Japan, buildings standing near cliffs suffered considerable damages, while buildings locating some distance from the cliffs sustained no damages. It has been suggested that such damages are due to large amplification of seismic waves associated with local topography and superficial soil properties.

This problem has been studied by numerous authors. Bouchon (Ref. 1) investigated the case of SH, P and SV waves on several types of topography by the approximation method developed by Aki and Larner (Ref. 2). Using an integral equation method, Wong and Trifunac (Ref. 3) studied the problem of scattering SH waves by semi-cylindrical and semi-elliptical canyons. Wond (Ref. 4) studied the problem of the diffraction of P, SV and Rayleigh waves by an elliptical canyon and a circular canyon solution of line sources in a half-space. On the other hand, other numerical solutions such as the finite difference method proposed by Alterman and Karal (Ref. 5) and Boore (Ref. 6) et al. and the finite element method by Smith (Ref. 7) et al., are also applied to problems of elastic wave propagation. In the present paper, the effect of topography and subsurface inhomogeneity on surface motion is investigated in the case of incident SV waves and Rayleigh waves with a new hybrid method combining a particle model with a finite element method. Several types of topography, such as cliffs with and without a soft layer at the foot of the slope are considered.

(I) Research Engineer and (II) Manager, Ohsaki Research Institute of Shimizu Construction Co., Ltd., Tokyo, Japan

Fundamental Wave Equations

Let us write the equations of motion in the x-y plane elastic medium as:

$$\rho\partial^2u/\partial t^2 = (\lambda + 2\mu)\partial^2u/\partial x^2 + (\lambda + \mu)\partial^2v/\partial x\partial y + \mu\partial^2u/\partial y^2$$
$$\rho\partial^2v/\partial t^2 = (\lambda + 2\mu)\partial^2v/\partial y^2 + (\lambda + \mu)\partial^2u/\partial x\partial y + \mu\partial^2v/\partial x^2 \qquad (1)$$

u and v are the components of displacement in the x and y directions respectively, ρ is the density and λ and μ are Lame's constants. Lame's constants are often replaced with other parameters such as:

$$\lambda = \frac{\nu E}{(1 + \nu)(1 - 2\nu)} \qquad \mu = \frac{E}{2(1 + \nu)}$$

Where E is Young's and ν is Poisson's ratio.

Particle Model Scheme

As shown in Fig. 1, let x and y be two dimensional cartesian coordinates and let h denote the grid increment. The grid point is denoted by (i,j). The mass is concentrated at every grid point. The following equations can be obtained (Ref. 8).

$$u(i,j,n+1)=2u(i,j)-u(i,j,n-1)+(C_L^2-C_T^2)k^2/h^2[u(i+1,j)-2u(i,j)+u(i-1,j)]$$
$$+((C_L^2-C_T^2)/4)k^2/h^2[v(i+1,j+1)-v(i+1,j-1)-v(i-1,j+1)+v(i-1,j-1)]$$
$$+(C_Tk/h)^2/2[u(i+1,j+1)+u(i+1,j-1)+u(i-1,j+1)+u(i-1,j-1)-4u(i,j)] \qquad (2)$$

$$v(i,j,n+1)=2v(i,j)-v(i,j,n-1)+(C_L^2-C_T^2)k^2/h^2[v(i,j+1)-2v(i,j)+v(i,j-1)]$$
$$+((C_L^2-C_T^2)/4)k^2/h^2[u(i+1,j+1)-u(i+1,j-1)-u(i-1,j+1)+u(i-1,j-1)]$$
$$+(C_Tk/h)^2/2[v(i+1,j+1)+v(i+1,j-1)+v(i-1,j+1)+v(i-1,j-1)-4v(i,j)] \qquad (3)$$

Let k and n denote the time increment and the time step, C_L and C_T are the compression and shear velocities, respectively. The time nk in Eqs. (2) and (3) is omitted.

Finite Element Method

Using a finite element method, Eq. (1) is rewritten in matrix form as:

$$[M]\{\ddot{u}\} + [K]\{u\} = 0 \qquad (4)$$

Approximating the derivatives in Eq. (4) by centered finite differences, Eq. (5) can be expressed in the form

$$\{u\}_{n+1} = 2\{u\}_n - \{u\}_{n-1} - [M]^{-1}[K]\{u\}_n \Delta t^2 \qquad (5)$$

$\{u\}$: nodal displacement vector $[M]$: lumped mass matrix
$[K]$: stiffness matrix t: time increment n: time step

Combining the FEM with the Particle Model

In this present paper, the respective merits of the particle model and the FEM are utilized by combining the two (Ref. 8,9). As shown in Figure 2, the FEM is applied to the internal boundary and the complex topography zone to avoid the problem of the boundary treatment. Further, in order to shorten computing times, reduce the required capacity of the computer and simplify data preparation work, the FEM is used for irregular zones only and the particle model is applied to other zones.

Wave Propagation in Irregular Ground due to Rayleigh Waves

In order to clarify the wave propagations in a two-layered ground with an inclined interface, one wave-length ($\lambda/h=2$, λ:wave-length, h:height of cliff) of Rayleigh waves of sine waveform was used and no damping of layers was considered in the following analyses (Ref. 10).

Illustrated in Fig. 3, when a Rayleigh wave propagates through a hard layer from the right to the left and it reaches the slope, it is divided into Rayleigh waves having two different phase velocities. These propagate further to the left through a two-layered ground. In order to investigate distribution of these Rayleigh wave amplitudes, the horizontal and vertical modes of R0 and R1 waves obtained by this analysis were plotted in Fig. 4. In this figure solid and dotted lines indicate modes determined by Haskell's method, assuming a uniform two-layered ground. It is seen that the R0 wave practically coincides with the fundamental mode obtained analytically, and the R1 with the first mode. When the phase velocity is obtained from the delay in propagation of waves, as shown in Fig. 5, the R0 wave coincides with the phase velocity for the frequency 2Hz($\lambda/h=2$) on the dispersion curve of the fundamental mode, while the R1 wave corresponds with the phase velocity of the first mode.

Amplification and Attenuation at Irregular Ground

In order to investigate the effect of topography and subsurface inhomogeneity on surface motion, Rayleigh waves with a sinusoidal waveform were considered, and the maximum displacements occurring at various points on the surface were investigated. In these cases the incident waves were assumed to have horizontal displacements of a unit amplitudes on the surface.

Figure 6 shows the maximum displacements at various points on the surface for $\lambda/h=4$ (λ:wavelength, h: height of cliff) and $\lambda/h=2$. Since Rayleigh waves propagate from the back of the slope, the amplitudes around top of the slope are fairly large. Particularly in the case of short wave-length (λ/h

=2) the vertical amplitude is at least three times as large as the horizontal amplitude of the incident wave, while in the case of $\lambda/h=4$, it is about 2.5 times the incident amplitude. In both cases the vertical movement is also predominant in the vicinity of the top of the cliff. There is also a periodic variation in maximum aplitudes along the ground surface at a distance from the top of the slope. These results are probably due to the effect of free surface and the interference of the reflected Rayleigh waves from the slope. Meanwhile, the large amplification are not seen at the ground below the cliff.

Figure 7 shows the maximum displacements at various points on the ground surface when Rayleigh waves propagate from the hard single-layered ground to the soft two-layered ground. Rayleigh waves propagating through the hard ground increase their amplitudes when they enter the two-layered ground having a soft surface layer. Further propagating in the two-layered ground at a certain distance from the sloping, waves of low propagation velocities are overlapped by waves of high velocities, and large amplitudes are produced. With an λ/h of 4, the vertical amplitude at the surface of the two-layered ground is about 2.5 times the horizontal amplitude of the incident waves. With an λ/h of 2, amplification is much larger compared to that of $\lambda/h=4$, and the vertical amplitude is more than five times larger than that of incident wave. The group velocities of the two-layered ground are shown in Fig. 8. From this graph, it is shown that the group velocity for the fundamental mode indicates a minimal value (airy phase) in the vicinity of 1.6Hz. The group velocity for 2Hz ($\lambda/h=2$) is extremely close to this minimal value compared with the case of 1Hz ($\lambda/h=4$). It is thought that 2Hz ($\lambda/h=2$) has a larger amplitude than $\lambda/h=4$ due to the influence of the airy phase near 1.6Hz.

Comparison of Responses of SV Waves and Rayleigh Waves

The maximum displacements at various points on the surface, when SV waves are vertically incident are shown in Fig. 9 and 10 compared with cases of Rayleigh waves, where SV waves were considered having horizontal displacements of a unit amplitude as incident waves.

Figure 9 shows maximum values of both Rayleigh and SV waves are produced near the top of the cliff. However in the case of a short wavelength ($\lambda/h=2$), the amplitude is larger for the Rayleigh wave than for the SV waves. In the case of a long wave-length ($\lambda/h=4$), amplitude of two waves are of almost the same value. In the case of Rayleigh waves, the vertical and horizontal amplitudes in the vicinity of the cliff are of roughly the same value and predominant. In the case of SV waves both horizontal and vertical amplitudes are predominant near the cliff.

Figure 10 shows maximum displacements for the SV and Rayleigh waves occur in the two-layered ground at a slight distance from the sloping interface. In the case of a long wave-length ($\lambda/h=4$), the maximum displacements for SV waves is about 1.5 times that for Rayleigh waves. However, when the wavelength is short ($\lambda/h=2$), the maximum value for Rayleigh waves is conversely about 1.5 times that for the SV waves. The dynamic characteristics of the ground motion for Rayleigh waves are different from those for SV waves, which is very interesting.

Up to this point only harmonic waves are considered in the analyses. Here the dynamic behavior of irregular ground are studied using actual seismic waves. It is impossible to separate the component of Rayleigh waves from recorded seismic waves. Therefore, in this study, the vertical components of the strong motion accelerograms of the Tokachi-oki Earthquake observed at Hachinohe, is assumed as the vertical component of Rayleigh waves.

Figure 11 shows the calculated displacements near the vicinity of the cliff. The maximum displacement along the ground surface is also shown in Fig. 12. From this diagram, the responses in the vicinity of the cliff show large amplifications of two to three times the amplitude of incident waves, and these the maximum values are similar to those for harmonic waves ($\lambda/h=4$) shown in Fig. 6.

Conclusion

The influences of irregular ground on SV waves and Rayleigh waves differ depending on the relationship between the incident wavelength and the geometrical dimensions of the irregular ground, and these influences cannot be ignored. Since Rayleigh waves with a large vertical amplitude are apt to predominate, a large displacement amplitude will be produced in irregular ground during a major earthquake. It will be necessary for thorough consideration to be given to the influence of topography on structures standing in the vicinity of irregular ground, especially pipe lines and nuclear power stations.

References

1. M. Bouchon. 'Effect of topography on surface motions', Bull. Seism. Soc. Am., Vol. 63, 615-632. (1973)
2. K. Aki and K.L. Larner. 'Surface motion of a layered medium having an irregular interface due to incident plane SH-waves', J. Geophysical Res., Vol. 75, 933-954. (1970)
3. W.L. Wong and M.D. Trifunac. 'Scattering of plane SH-wave by a semi-elliptical canyon', Earthquake Eng. and Struct. Dyn., Vol. 3, 157-169. (1974)
4. H.L. Wong. 'Effect of surface topography on the diffraction of P, SV and Rayleigh waves', Bull. Seism. Soc. Am., Vol. 72, 1167-1183. (1982)
5. Z. Alterman and F.C. Karal. 'Propagation of elastic waves in layered media by finite difference methods', Bull. Seism. Soc. Am., Vol.63, 615-632. (1968)
6. D.M. Boore. 'A note on the effect of simple topography on seismic SH-waves'. Bull. Seism. Soc. Am., Vol. 62, 275-284. (1972)
7. W.D. Smith. 'The application of finite element analysis to body wave propagation problems', Geophys. J.R. Astro. Soc., Vol.42, 747-768. (1975)
8. A. Ohtsuki and K. Harumi. 'Effect of topography and subsurface inhomogeneities on seismic SV waves', Earthquake Eng. and Struct. Dyn.,

Vol.11, 441-462. (1983)

9. A. Ohtsuki, H. Yamahara and M. Hirose, 'Computer simulation of elastic waves near a foundation through use of a new analytical model', Shimizu Tech. Res. Bull., Vol.1, 19-27. (1982)
10. A. Ohtsuki, H. Yamahara and K. Harumi, 'Effect of topography and subsurface inhomogeneity on seismic Rayleigh waves', Earthquake Eng. and Struct. Dyn., (to be published) (1984)

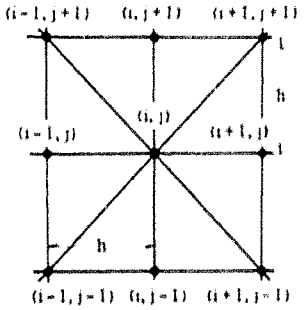

Fig. 1 Particle model grid.

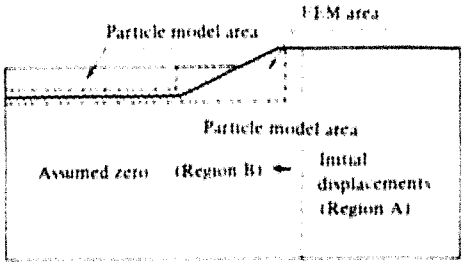

Fig. 2 Analytical model combining FEM with particle model and locations of initial displacements.

Table 1 Soil properties

	Model 1	Model 2	
		Surface layer	Underlying half-space
Shear velocity (m/s)	200	100	200
Compressional velocity (m/s)	600	300	600
Density (g/cm³)	1.6	1.6	1.6

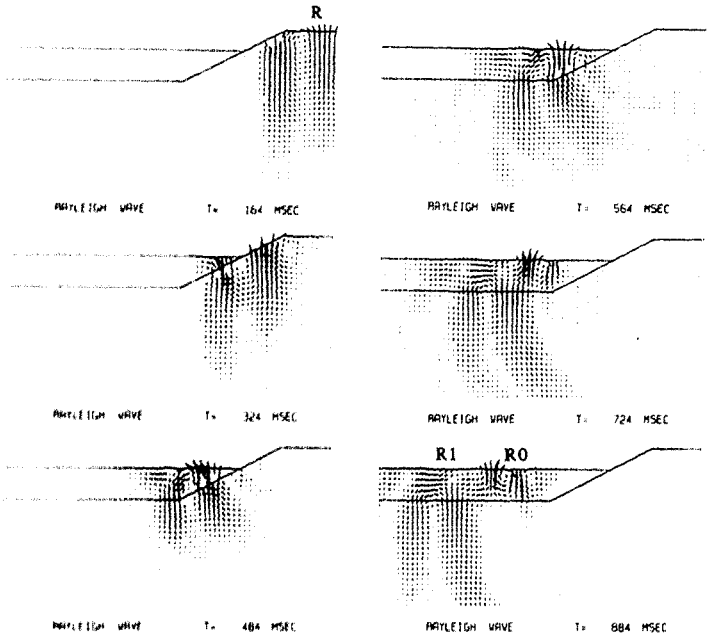

Fig. 3 Wave propagation near cliff with a soft layer due to Rayleigh wave.
R: Incident Rayleigh wave.
R0: Transmitted wave with fundamental mode.
R1: Transmitted wave with first mode.

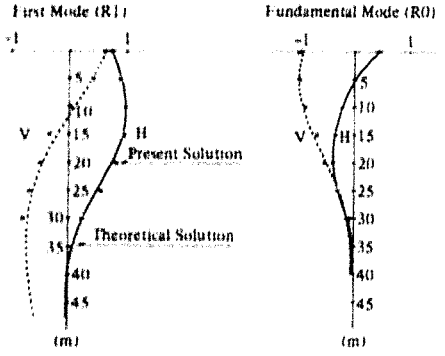

Fig. 4 Shapes of first two Rayleigh modes for a soft layer of 30m thick overlying a half-space obtained by Haskell model, and present solutions.

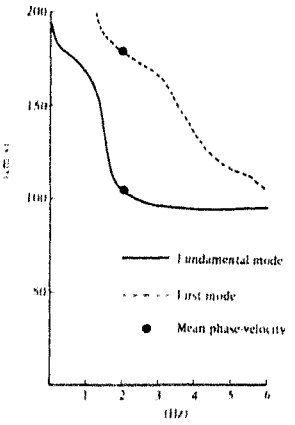

Fig. 5 Phase-velocity curves of Rayleigh wave for a soft layer of 30m thick overlying a half-space obtained by Haskell model, and mean phase-velocity obtained by present method.

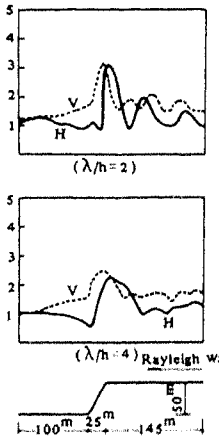

Fig. 6 Distributions of maximum horizontal and vertical surface displacements by harmonic Rayleigh waves for λ/h=2 and λ/h=4. (h=50m)

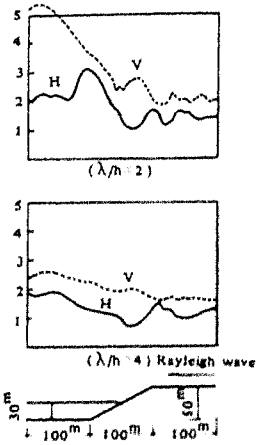

Fig. 7 Distributions of maximum horizontal and vertical surface displacements by harmonic Rayleigh waves for λ/h=2 and λ/h=4. (h=50m)

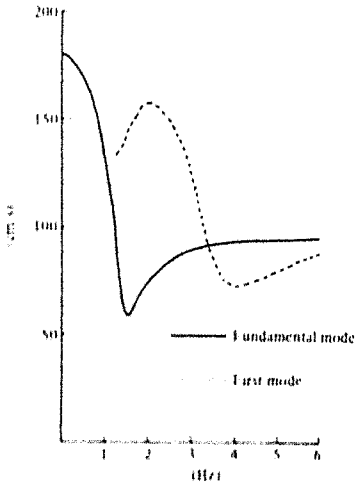

Fig. 8 Group velocity curves of Rayleigh wave for a soft layer of 30m thick overlying a half space obtained by Haskell model.

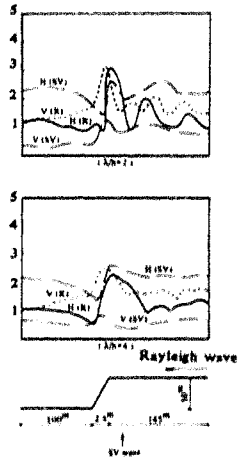

Fig. 9 Distributions of maximum horizontal and vertical surface displacements by harmonic SV waves and Rayleigh waves

H(SV) horizontal displacement due to SV wave
V(SV) vertical displacement due to SV wave
H (R) horizontal displacement due to Rayleigh wave
V (R) vertical displacement due to Rayleigh wave

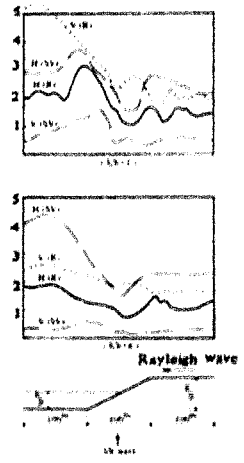

Fig. 10 Distributions of maximum horizontal and vertical surface displacements by harmonic SV waves and Rayleigh waves

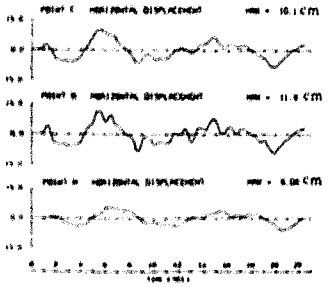

Fig. 11 Horizontal displacements at points (A, B, C) near cliff subjected to Tokachi-oki Earthquake.

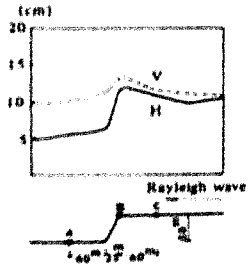

Fig. 12 Distribution of maximum horizontal and vertical surface displacements subjected to Tokachi-oki Earthquake.